Results in Engineering 27 (2025) 106191

Contents lists available at ScienceDirect

Results in Engineering

journal homepage: www.sciencedirect.com/journal/results-in-engineering

Research paper

Turning marine microplastics into components for producing innovative bituminous mastics: Boosting sustainability in road pavements

Yanqi Wang [a,b,1], Rosa Veropalumbo [c,1], Federica Recupido [a,1], Cristina Oreto [c], Quansheng Sun [d], Letizia Verdolotti [a,*], Assunta Campanile [e], Barbara Liguori [e], Nunzio Viscione [c], Gianluca Dell'Acqua [c], Francesca Russo [c,*], Giuseppe Cesare Lama [a]

[a] Institute for Polymers, Composites and Biomaterials, National Research Council of Italy, P.le E. Fermi 1, 80055, Portici, Italy
[b] School of Automotive Engineering, Hebei Petroleum University of Technology, Chengde City, Hebei Province, 067000, China
[c] Department of Civil, Construction and Environmental Engineering, University of Naples, Federico II, Via Claudio 21, 80125, Naples, Italy
[d] School of Civil Engineering and Transportation, Northeast Forestry University, Harbin, 150040, China
[e] Chemical, Materials and Industrial Production Engineering (DiCMaPi), University of Naples, Federico II, Piazzale Tecchio 80, 80125, Naples, Italy

ARTICLE INFO

Keywords:
Microplastics
Bituminous mastics
Rheological properties
Leaching Test
Environmental Assessment
LCA analysis

ABSTRACT

Marine-microplastics pose a significant environmental threat due to their accumulation, which causes irreversible damage to marine ecosystems and wildlife. However, these same microplastics can be repurposed to enhance the performance of asphalt mastics, improving road durability and promoting recycling. This study investigates the feasibility of using marine-microplastics as modifiers in two types of bituminous mastics, at a concentration of 6wt %. These include the conventional black neat bitumen (for road pavements) and a more sustainable, transparent Albino bitumen (for pedestrian pavements). The modified mastics are characterized by a range of physical-rheological, chemical, morphological, and thermal properties. The potential for plastic leaching is evaluated by simulating acid rain conditions (pH≤5.6). Additionally, a Life-Cycle-Assessment methodology is applied to quantify the Climate Change indicator for 1m² of road pavement using the obtained mastics. Results show that incorporating marine-microplastics improves the mechanical and rheological properties of bituminous mastics; in fact, this latter shows a softening point improvement of 9.8 °C compared to the neat bitumen (46 °C) and at the same time the addition of marine-microplastics into neat bitumen produces a stiffness reinforcement by over 80 % compared to the conventional mastic. Furthermore, leachate heavy metal concentrations decrease by up to 85 %, for Cd, which reduces from 14 mg/kg (neat bitumen) to 2mg/kg, by employing marine-microplastics. Notably, the climate change indicator is reduced by up to 16 % compared to traditional solutions, attributed to the extended service life provided by marine-microplastics in the mastics. This study presents a promising recycling strategy, offering a sustainable solution for road engineering applications.

Abbreviation list

$a(T)$	Shift factor at T
$a(T_0)$	Shift factor at T_0
ABS	Acrylonitrile Butadiene Styrene
ALB	Albino Bitumen
ATR-FTIR	Attenuated Total Reflectance Fourier Transform Infrared
B50:70	Bitumen with pavement grade 50/70
CC	Climate Change
Cd	Cadmium
CO_2	Carbon Dioxide
Cr	Chromium
DSC	Differential Scanning Calorimetry
DSR	Dynamic Shear Rheometer
DTGA	Derivative Thermogravimetric Analysis
EN	European Standards
FTIR	Fourier Transform InfraRed
G*	Complex Shear Modulus
HDPE	High-Density Polyethylene
HMPs	High Melting Point Microplastics

* Corresponding authors.
E-mail addresses: letizia.verdolotti@cnr.it (L. Verdolotti), francesca.russo2@unina.it (F. Russo).
[1] These authors equally contributed to this work.

https://doi.org/10.1016/j.rineng.2025.106191
Received 22 April 2025; Received in revised form 5 July 2025; Accepted 8 July 2025
Available online 9 July 2025

HNO_3	Nitric acid
ICP	Inductively Coupled Plasma
IPC-MS	Inductively Coupled Plasma Mass Spectrometry
LCA	Life Cycle Assessment
LDPE	Low Density Poly Ethylene
LLDPE	Linear Low Density Poly Ethylene
LMPs	Low Melting Point Microplastics
LP	Limestone Powders
MMPs	Medium melting point microplastics
Mo	Molybdenum
MPs	Microplastics
Ni	Nichel
PACs	Polycyclic Aromatic Compounds
PAHs	Polycyclic Aromatic Hydrocarbons
Pb	Lead
PE	Polyethylene
PES	Polyether sulfone
PET	Polyethylene terephthalate
POM	Polarized Optical Microscopy
PP	Polypropylene
PS	Polystyrene
PVC	Polyvinyl chloride
SARAs	Saturated Hydrocarbons, Aromatics, Resins, and Asphaltenes
SBR	Styrene Butadiene Rubber
SM	Supplementary Materials
TGA	Thermogravimetric Analysis
T	Shift Temperature
T_g	Glass Transition Temperature
$Tmax$	Maximum Degradation Temperature
T_0	Reference Temperature (20°C)
$T_{onset,}$	Onset Degradation Temperature
Vis	Visible Light
UV	Ultraviolet

1. Introduction

Over the past decades, the accumulation of huge amounts of plastic waste in soil and mainly in the oceans (and in general waterways) has become a global issue [1]. On this account, it has been estimated that 400 million tons of plastic waste in 2022 were produced, whereas 0.5 % was leaked into the oceans and coastlines [2]. Among plastic waste, microplastics (namely MPs), conventionally defined as particles with sizes lower than 5 mm [3–5] are obtained from the fragmentation of synthetic polymer debris (either thermosets [6] or thermoplastic materials), such as polypropylene (PP), polyethylene (PE), polyvinyl chloride (PVC), polyether sulfone (PES) resin, polyethylene terephthalate (PET), polystyrene (PS) and styrene-butadiene rubber (SBR) [7]. MPs are usually obtained by the mechanical action of ocean waves as well as chemical/physical processes such as UV irradiation [8], photodegradation [9] or biological activities (i.e. biofouling) [10–12]. Several sources can lead to the formation of marine micro- and macro-plastics, such as surface runoff, wastewater from sewage treatment plants, aquaculture, and fisheries, or industrial wastes [13,14]. Such processes usually give rise to so-called "*secondary microplastic systems*", which differ from primary ones, which are byproducts of particulate emissions of industrial production [15]. Because of their stable chemical structure, which can persist in the ocean for hundreds of years [16], MPs are extremely harmful to marine wildlife. Moreover, they contain additives or act as carriers for pollutants, provoking uptake in marine ecosystems and thus leading to chronic toxicity [17–19]. This phenomenon seriously threatens marine ecosystems at different trophic levels and consequently human health [20]. Thus, removing the current MPs pollution from water bodies and coastal environments has become a global concern, being included as the 14th Sustainable Development Goal by the United Nations [21] to be reached within 2030. Governmental policies and actions are required to address MPs pollution in the short term. Millions of tons of plastic debris and MPs have already been removed from oceans, seas, and rivers [22,23] using different solutions, including barriers and cleaning vessels [24,25]. Scientific efforts have been dedicated to assessing the economic feasibility of such activities, taking into account both the costs of MP removal and the benefits that this activity provides to society, demonstrating that several techniques can meet the willingness to pay of governmental organizations [26]. Other studies [27] evaluated the life cycle costs of collecting, storing, transporting, sorting, shredding, and cleaning waste plastics removed from the ocean, including MPs; they concluded that several recycling scenarios ended up with a positive economic outcome. The current recycling routes of MPs include physical and chemical methods. In the first case, sorting, washing, and grinding, followed by density separation, sieving, filtration, and precipitation are typically selected [28]. Although mechanical recycling is more advantageous in terms of energetic inputs, MPs still need to be further purified [29]. In contrast, chemical methods usually involve the conversion of polymers into monomers or oligomers, reused in industrial production chains as fuels or raw materials through pyrolysis [30,31] or catalytic decomposition [32] aiming at energy recovery. Other routes based on glycolysis, hydrolysis, aminolysis [33], or photocatalysis have been also indicated in the literature. Recently, biotechnological processes based on enzymes and microorganisms enabling to depolymerize MPs have also gained remarkable attention [34]. However, not all MPs that are removed from the environment can be effectively reused, and in most cases, they end up in incinerators or landfills [35–37]. Therefore, it is worth exploring eco-friendly ways to reuse MPs to reduce their diffusion and accumulation into the marine environment. On this account, a possible eco-friendly strategy to reintegrate some MPs coming from post-consumer or post-industrial streams such as PET [37–40] LDPE [41], HDPE [42], PVC [43] PP [44,45] to be used as modifiers into bitumen to enhance the features of asphalt mastics, by complying the need of sustainability in the road engineering applications. It has been demonstrated that the use of MPs has positive effects on bitumen final performance such as reducing penetration, increasing softening point [46], improving elastic recovery [47], reducing permanent deformation [39], and improving thermal stability [46]. Moreover, the addition of MPs also might be long-term performing pavements and thus reducing the maintenance cycles as well as economically more viable with respect to the virgin materials [48,49]. Usually, MPs might be incorporated within bitumen through both wet and dry processes. The first case involves the pre-mixing of MPs with bitumen to replace part of bitumen at elevated temperatures. Dry processes enable to add MPs to partially replace aggregates within bitumen [50]. Nevertheless, the evaluation of the environmental effects of the dispersion of MPs into asphalt pavements has not completely explored in the literature.

Veropalumbo et al. [51] argued that the encapsulation of the micro and nano plastics based on PET and LDPE from packaging bags at different concentrations (5 %, 10 %, and 20 %) into the bitumen mastics reduced the potential release of micro- or nano- plastics in water by >99 %. In addition, the MP incorporation led to a 20 % improvement in the bitumen stiffness compared to that of conventional limestone-reinforced asphalt mastics. Subsequently, the same authors selected a mixture of MPs based on HDPE, LDPE, PP, and PET from recycling plants to be used in bituminous systems, evaluating their environmental performances through Life Cycle Assessment (LCA). The resulting modified bitumen systems presented more elastic properties (30 % increase) than the conventional limestone-modified systems, displaying a reduction by 85 % of the emissions of nitrogen, sulfur, and phosphorus compounds into water as well as longer life service and lower endpoint indicators (34 % reduction) [27].

It is important to point out that MPs added to bituminous mastics might affect the leaching of organic pollutants and/or heavy metals from asphalt roads when they come into contact with rainwater. For this reason, it is mandatory to validate such materials in terms of leaching performances in adverse environments, such as acid rains (i.e., rainfall,

snow, hail, fog, dew, and other atmospheric precipitation with pH value $\leq$ 5.6). Nonetheless, the environmental impact of using MPs for mastic modification and their application in pavement construction has recounted controversial results [46,48,51,52]. In the work of Enfrin et al., the release of LDPE/LLDPE and Acrylonitrile butadiene styrene (ABS) MPs from asphalt was investigated simulating scenarios of road traffic abrasion, whereas MPs leaching was dramatically enhanced by cold and acid conditions [53]. Järlskog et al., investigated the emission of MPs from road pavements, demonstrating the highest accumulation of plastic waste through storm and wash waters [54]. To the best of the authors' knowledge, MPs from marine environments as a modifier in bituminous mastics have never been explored before. Hence, the objectives of this study are: (1) to clarify how marine MPs (a blend of PP, LDPE, and LLDPE) influence the mechanism of an albino bituminous solution and the underlying modification, (2) to assess their potential release from bituminous mastics to the environment when exposed to rainfall i.e., acid rain. (3) to evaluate the environmental impact of the selected modified systems. Six plastic MPs-modified mastics are prepared and characterized. Two neat bitumen and two conventional limestone powder-filled mastics are tested as controls. Two model bituminous systems are selected: a conventional black B50/70 bitumen (B50/70), widely used for hot mastics for road pavement applications [55] and a more sustainable transparent bitumen named Albino bitumen (ALB), widely used for light-colored pavements to control the light absorption and thermal energy storage in asphalt pavements [56]. The feasibility of marine MPs as a modifier is explored by physical (softening point and penetration) and rheological properties (master curves and Black diagram). The thermal, chemical, and morphological properties are then selected to characterize the effect of MPs on bituminous mastics characteristics. The leaching of MPs into the environment by simulating acid rain is assessed through a custom-made test, able to quantify the concentration of released heavy metals. Organic Saturated Hydrocarbons, Aromatics, Resins, and Asphaltenes (SARAs) released from the modified bituminous systems [57] are also assessed through spectrophotometric techniques. Finally, an LCA is applied to quantify life cycle sustainability indicators related to the substitution of the limestone filler with recycled MPs in asphalt mastics for road pavement applications.

2. Experimental

2.1. Materials

2.1.1. Modifiers: MPs and limestone powder

MPs, derived from the milling of collected plastic containers on the beaches of the Tyrrhenian Sea, consist of a mixture of PP, LDPE, LLDPE (Fig. S1, grading curve shown in Fig. S2, Section S1, supplementary materials, S.M.) with a maximum size around 1 mm. This mixture namely (MMPS) is used as the additive for the production of the mastics; the same mixture is dived on the bases of different melting point obtaining other two different plastic additive as follows: (1) high melting point -MPs (namely HMPs) associated with PP with melting point of 163 °C, and (2) low melting point-MPs correlated to the PE-based plastic materials, LDPE and LLDPE, with melting point of 112 °C and 126 °C respectively (namely LMPs). The selected MPs undergo a washing process to remove sulfate derived from seawater before subjecting them to milling. Differential Scanning Calorimetry (DSC) thermo-grams and Fourier Transform InfraRed (FTIR) spectrum for each MPs category are shown in Fig. S3 and Fig. S4 (S.M.). Thermal properties of the selected MPs are resumed in Table S1 (S.M.).

Limestone powders (LP) with a specific gravity of 2.737 g/cm^3, Rigden voids of 41.44 %, and a specific surface area of 5480 m^2/g [51,52] are employed as modifiers for bitumen for comparison purposes.

2.1.2. Binders

Neat 50/70 (B50/70) and ALB bitumen are used as binders in this study, whose properties are summarized in Table 1.

2.2. Bituminous mastic preparation

For the preparation of MPs-modified bituminous mastics, a high-speed shear dispersion apparatus is employed, whereas MPs are uniformly dispersed through high-speed rotating paddles. The viscoelasticity state of the base bitumen is evaluated since the bitumen and the molten polymer particles might have physical or chemical interactions with each other at high temperatures. The MPs-modified bituminous mastics are prepared according to a four-step procedure (Fig. S5, Section S2, S.M.):

I. The binders (B50/70 and ALB bitumen) are preheated in an oven at 150 °C for 30 min.
II. Bitumen is then poured into a clean metal box and located onto a temperature-controlled heating device to ensure a constant temperature of 165 °$C \pm 5$ °C.
III. MPs are then added at 6 wt. % of the mass of the bitumen and dispersed in bitumen at 165 °C for 30 min at 600 rpm to ensure a good dispersion. This parameter confirms that MPs are molten and phase separation is minimized. Moreover, 6 wt. % represents the optimal concentration at which degradation phenomena are minimized.
IV. The resulting mastics are then transferred into a new metal box for 24 h.

A total of six MPs modified-mastics are prepared. The limestone-based mastics are formulated in the same way. Conclusively, a total of eight bituminous mastics are obtained: two limestone-modified mastics (B50/70 + 6 % LP and ALB + 6 % LP) and six MPs-modified-mastics (namely B50/70 + 6 % HMPs, B50/70 + 6 % MMPs, B50/70 + 6 % LMPs, ALB + 6 % HMPs, ALB + 6 % MMPs, ALB + 6 % LMPs).

2.3. Methods

2.3.1. Basic and rheological characterization

Softening point and penetration tests are carried out, respectively, following the EN 1427 and EN 1426 standards. Results are shown as average and standard deviation of three independent measurements.

Frequency sweep test is selected to characterize the rheological performance of bituminous mastics through a Dynamic Shear Rheometer (DSR, Anton Paar Smart PAVE 102) at defined temperatures (−10 °C, 0 °C, 10 °C, 20 °C, 30 °C, 40 °C, 50 °C and 60 °C) in the frequency range of 0.1 Hz to 10 Hz (considering a total of 20 measurement points, with intervals of 0.1 for frequencies from 0.1 to 1 Hz and 1 Hz for frequencies from 1 to 10 Hz, passing through 1.59 Hz) according to EN 14,770 standard. Specifically, a plate-to-plate system with a 25 mm diameter and a gap of 1 mm is used for test temperatures equal to and above 30 °C, while a diameter of 8 mm with a gap of 2 mm is adopted for test temperatures below 30 °C.

Master curves are then acquired according to the William-Landel-Ferry equation (Eq. (1)) with 20 °C as a reference temperature. To analyze the viscoelastic behavior of different mastics, Black diagrams are employed.

Table 1
Physical properties of the examined bitumen.

Properties	Standard method	B50/70	ALB
Penetration at 25 °C (dmm)	EN 1426	62	54
Softening point (R&B) (°C)	EN 1427	46	69
Dynamic viscosity at 150 °C (Pa•s)	EN 13,702	0.36	0.42
Dynamic viscosity at 100 °C (Pa•s)		4.40	9.74
Dynamic viscosity at 60 °C (Pa•s)		276	5406

$$\log \frac{a\ (T)}{a\ (T_0)} = \frac{-C_1 \cdot (T - T_0)}{C_2 + T - T_0} \quad (1)$$

T_0 is the reference temperature (20 °C), T is the shift temperature (°C); $a(T)$ and $a(T_0)$ are shift factors at T and T_0, respectively; C_1 and C_2 are constants, determined by regression of experimental data.

2.3.2. Morphological, chemical and thermal characterization

The morphology of the modified bituminous mastics is assessed through Polarized Optical Microscopy (POM, Zeiss Axioskop microscope, Germany). Before imaging, a glass coupon is placed onto a heated stirrer at 100 °C; then a few milligrams of samples are poured onto the top of the glass coupon and positioned between two coverslips to form a thin film. Subsequently, specimens are cooled down to 30 °C. Images are then acquired by crossed polarizers and a CFW-1312C Digital Camera at different magnifications [58].

Attenuated Total Reflectance Fourier Transform Infrared Spectroscopy (ATR-FTIR, Perkin Elmer Spectrum 100 series spectrophotometer, Waltham, MA, USA) is used to investigate the modification mechanism of MPs on bituminous mastic chemical characteristics. Spectra are recorded in transmittance mode with a resolution of 4 cm^{-1}, within a wavenumber range from 4000 cm^{-1} to 600 cm^{-1} with 32 scans.

The thermal properties of the modifiers (both MPs and LP) and bituminous mastics are evaluated by DSC (Discovery DSC 2500, Waltham, MA, USA). Three scans are performed: from-70 °C to 200 °C, then cooled from 200 °C to −70 °C, and finally heated from −70 °C to 200 °C again, using an increase rate of 10 °C min^{-1} under nitrogen flow (50 mL min^{-1}) [59,60]. The first scan is meant to eliminate the thermal history, the second to cool the system down to obtain the crystalline behavior, and finally, the third heating scan to examine the melting behavior. The thermo-degradative behavior of the examined systems is assessed through Thermogravimetric analysis (TGA) and Derivative Thermogravimetric analysis (DTGA). Experiments are carried out using TA Q5000 balance (TA Instruments, New Castle, DE, USA) under N_2 flow (volumetric flow rate = 40 mL min^{-1}) using a scanning rate of 10 °C min^{-1} from 30 °C to 800 °C.

2.3.3. Environmental assessment

The examined bituminous mastics undergo a custom-made leaching test, designed to simulate acid rainfall conditions. Toxic metal ions release is estimated by contacting under continuous stirring a suitable amount of each mastic (solid-to-liquid ratio by weight equal to 1/50) at room temperature with an acid solution (pH which is fixed at 4.0, adding suitable amounts of a 1 M HNO_3 solution). After filtration, the concentration of the most relevant toxic elements released is evaluated through Inductively Coupled Plasma (ICP) spectrometry (ISO 17,294–2:2003. Water quality - Application of inductively coupled plasma mass spectrometry (ICP-MS) - Part 2). Since bitumen is derived from crude oil refining processes, its chemical composition results in organic SARAs (Saturated Hydrocarbons, Aromatics, Resins, and Asphaltenes) and therefore Polycyclic Aromatic Compounds (PACs), which include hazardous contaminants such as Polycyclic Aromatic Hydrocarbons (PAHs). PACs and many other organic pollutants exhibit very specific ultraviolet-UV and/or Visible-Vis absorption spectra due to the presence of the chromophoric structure; therefore, UV–Vis spectroscopic analysis plays an important role in their detection. UV–Vis spectroscopy refers to analytical methods based on the measurement of the absorption or reflection of light by a substance in the wavelength range of 190–900 nm (UV range: 190–380 nm and visible range: 380–900 nm) [61]. Therefore, to assess the potential leaching of organic contaminants, water-based eluates coming from the above-mentioned leaching tests are characterized by UV–Vis analysis (Cary 60 UV–Vis, Agilent Technologies), by measuring absorbance in the range 200–800 nm. 1 mL of each solution is placed into a standard quartz cell with a 10 mm-optical path length and 1 M HNO_3 solution is used as blank.

2.3.4. Life cycle assessment

The LCA methodology is applied to quantify and compare the life cycle impacts of the bituminous mastics B50/70 + 6 % LP, B50/70 + 6 % HMPs, B50/70 + 6 % MMPs and B50/70 + 6 % LMPs. The methodological framework of LCA complies with EN 14,040 and EN 15,804; the system model and relative inventory and impact assessment are drafted using SimaPro 9® calculation tool [27]. To correctly model the LCA boundary, it is paramount to define the function of the product system; in the present analysis, the bituminous mastics are intended as the matrix that binds and coats the mineral aggregates that make up the solid skeleton of road construction materials, namely the hot asphalt mixtures. Hence, the LCA is carried out according to a "*cradle to grave*" approach, where the functional unit of the analysis is 1 m^2 of road pavement base layer, the deepest structural layer of a highway road pavement, analyzed through an analysis period of 20 years, the typical service life of a conventional base layer; in each scenario, the base layer is composed of a mixture of limestone coarse aggregates and sand bonded, in turn, with the 4 alternative hot asphalt mastic solutions here investigated, one for time: 1) B50/70 + 6 % LP, 2) B50/70 + 6 % HMPs, 3) B50/70 + 6 % MMPs and 4) B50/70 + 6 % LMPs (fixed the asphalt binder content by the weight of aggregates of each asphalt mixture, equal to 5 %, and the specific gravity of the asphalt mixture, equal to 2.4 g/cm^3). The service life of each alternative base layer is calculated according to the same methodology and boundary conditions applied in Russo et al. [27], in which the complex shear moduli of the asphalt mastics are used to forecast the asphalt mixtures' moduli [62]. The stress-strain state of the pavement multilayer is calculated. Damage accumulation equations are applied to predict the number of axle loads before any fatigue or rutting [63] occurs, triggering the road pavement end-of-life scenario. Fixed all the necessary boundary conditions, the service life of an 18 cm-thick base layer is equal to 20, 22, 22, and 24 years, for B50/70 + 6 % LP, B50/70 + 6 % HMPs, B50/70 + 6 % MMPs and B50/70 + 6 % LMPs, respectively.

Table S2 (Section S3, S.M.) summarizes the stages of the life cycle and the relative inventory data used in the analysis. The recycling processes of MPs were modelled based on literature data [64–66].

The life cycle impacts were quantified in terms of Climate Change (CC) indicator, calculated according to the impact assessment methodology EN 15,804 + A2 V1.00. The resulting life cycle impact indicators are allocated to the same analysis period (20 years) using as allocation criteria the residual economic value of the pavement [27].

3. Results and discussion

3.1. Basic and rheological properties

3.1.1. Basic properties evaluation

The softening point and penetration of B50/70 and ALB-modified bituminous mastics are depicted in Fig. 1.

Bituminous mastics with higher softening points and lower penetration levels are widely recognized for their superior resistance to defects caused by high temperatures [67].

LP dispersion induces a slight increase in the softening point of B50/70 bitumen from 46 °C to 49.2 °C (Fig. 1a). The softening point of B50/70 is improved by 6.1 °C, 8.0 °C and 9.8 °C by using HMPs, MMPs and LMPs, respectively (Fig. 1a). The softening point of ALB slightly increases (from 69 °C to 69.7 °C, Fig. 1b) by adding LP. In contrast to the case of B50/70 mastics (where B50/70+LMPs exhibits the highest softening point), ALB+HMPs shows the highest softening point (74.2 °C), followed by ALB+MMPs (73 °C) and ALB+LMPs (72.3 °C). A reduction of penetration of B50/70 (Fig. 1a) of 1.2 dmm, 8.0 dmm, 11.0 dmm and 17.4 dmm is observed by selecting LP, HMPs, MMPs, and LMPs.

The penetration of ALB+LP is only 0.6 dmm smaller than that of ALB. In contrast, the penetration of ALB (44.0 dmm) is reduced by 9.2 dmm, 7.0 dmm and 5.8 dmm by adding HMPs, MMPs, and LMPs, respectively

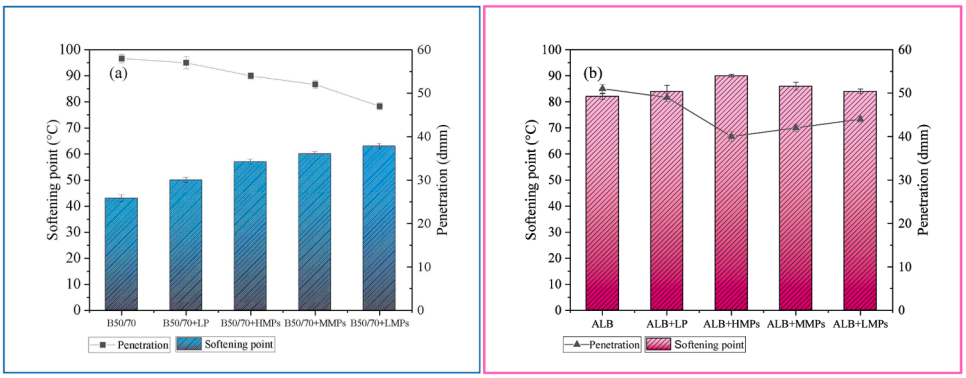

Fig. 1. Basic properties of MPs-modified mastics. a) Softening points of B50/70 (bar plot) and penetration (scatter-line plot) and b) Softening point of ALB mastics-based mastics (bar plot) and penetration (scatter-line plot). Results are expressed as average and standard deviation of three independent measurements.

(Fig. 1b). This might be ascribed to both the particle geometry effect of LP [68] and their physicochemical interaction with bitumen [69]. The bitumen thickness formed by the adsorption of polar components such as asphaltene on the mineral powder's surface contributes to the mastic's high stiffness [70,71]. Remarkably, the softening point and penetration of the examined MPs-modified bituminous mastics outperform the LP-modified mastics. This positive effect may be explained by the lower specific gravity and larger specific surface area of MPs compared to the case of LP [51]. The superiority of the physical properties of MPs-modified systems over those of LP-based ones is also attributed to the network structure formed by the molten MPs with bitumen components [72].

3.1.2. *Rheological characterization*

The master curves for examined bituminous mastics are shown in Fig. 2a and b, respectively, where, the complex shear modulus (G*) of all the mastics is reported against the reduced frequency. Usually, G* in the low-frequency range represents the high-temperature performance of asphalt mastic, while in the high-frequency range, it corresponds to the low-temperature performance.

For both cases, the deviation in G* compared to the neat mastics is most pronounced in the low and intermediate frequency domains. Within this range, the master curves for MPs-modified bituminous mastics consistently rise above those of LP-modified mastics as the reduced frequency decreases [73]. Observing the zone from intermediate to high-frequency range, the main curves of each mastic are gradually overlapped with the increase of reduced frequency; this indicates that both LP and MPs have a significant effect on the high-temperature properties of both the examined systems. Conversely, they have minimal impact on the rheological properties at low temperatures. Nevertheless, when employing MPs, the overall G* exceeds that of LP-modified ones, especially in high-temperature performance. Notably, in the frequency range of 1.0E-06 Hz to 1.0E-01 Hz, the G* of B50/70+LP is, on average, 2 % higher than that of B50/70. The increase of G* value for B50/70+LMPs is the most notable, showing a 593.3 % increase compared to neat B50/70. This is followed by B50/70+MMPs with a 156.4 % increase and B50/70+HMPs with an 81.6 % increase. In contrast, the most significant improvement in G* for ALB is achieved with HMPs. LMPs and LP have nearly the same impact on the G* of ALB, though the G* of ALB+LMPs is slightly higher than ALB+LP in the frequency range of 1E-03 Hz to 1E-06 Hz. This phenomenon is consistent with the softening point and penetration trend by employing the selected MPs (Fig. 1).

Black diagrams are devoted to analyzing the viscoelastic properties of the investigated systems (Fig. 3a and b).

The addition of LP at 6 wt % does not show a significant effect on the viscoelastic properties of B50/70 and ALB. In contrast, the addition of MPs shifts both the B50/70 and ALB curves to the right and downwards, especially in the low and intermediate reduced frequency ranges. The interaction between the molten MPs and bitumen alters its rheological properties, causing a decrease in phase angle and an increase in complex modulus, indicating enhanced elasticity. This effect is particularly pronounced at higher temperatures, such as in low-frequency ranges. It must be noted that the interaction between MPs and bitumen is often dominated by the composition of the bitumen as well as the physical/chemical properties of the MPs and their compatibility with the mastics [74]. Consequently, MPs-modified bituminous mastics show remarkable differences in viscoelastic behavior (Fig. 3a and b) whereas a distinct effect of MPs on the viscoelastic behavior of B50/70 and ALB-based mastics can be observed. Specifically, B50/70+HMPs exhibits a plateau at a phase angle of approximately 74°, corresponding to a G* value of 0.06 MPa (Fig. 3a). This plateau is further reduced with MMPs

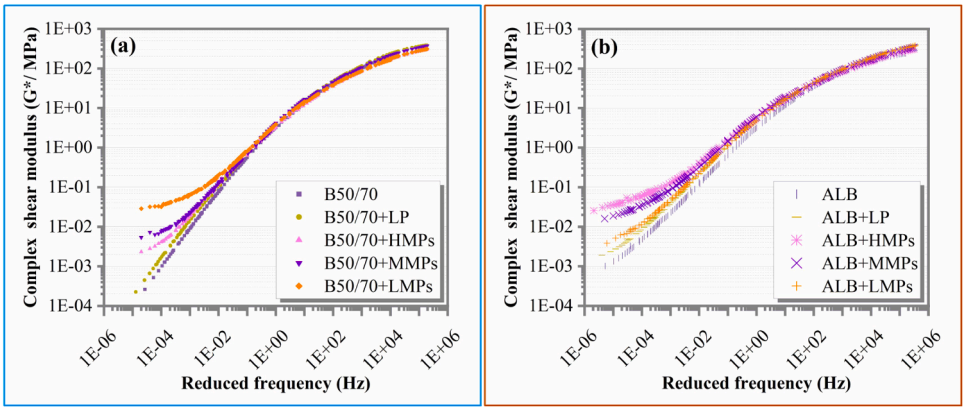

Fig. 2. Master curves of MPs-modified mastics, a) B50/70-mastics, b) ALB-mastics.

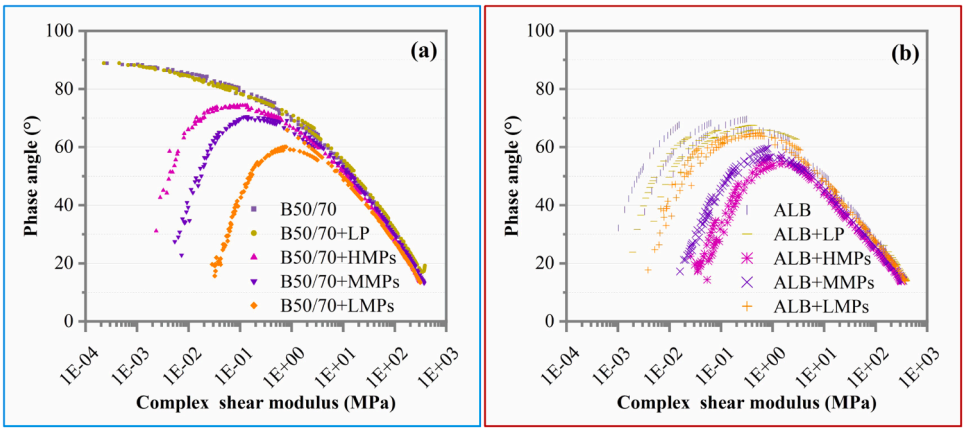

Fig. 3. Black diagrams of MPs-modified bituminous mastics, (a) B50/70-based and (b) ALB-based mastics.

and LMPs, showing a phase angle of 70° and a G* of 0.12 MPa for B50/70+MMPs, and a phase angle of 60° with a G* of 0.66 MPa for B50/70+LMPs.

ALB+HMPs evidences enhanced viscoelastic properties with a phase angle of about 56° corresponding to a G* of 0.90 MPa in the plateau region, which is followed by 60° corresponding to a G* of 0.8 MPa for ALB+MMPs and 65° corresponding to a G* of 0.32 MPa for ALB+HMPs (Fig. 3b).

From these results, it emerges how different types of plastic influence differently the behavior of a completely black solution from the albino one. Specifically, a plastic having a lower melting point makes the bituminous mastic reach performances comparable to those of a modified bitumen; differently, the addition of harder plastic, having melting points higher than the processing temperatures of the bituminous mastics, highlights the best properties by far. In any case, the introduction of any type of plastic in bituminous mastics is not only mechanically valid but also environmentally friendly.

3.2. Analysis of interaction between MPs and bitumen

3.2.1. Morphological analysis

The dispersion of MPs in the examined bituminous mastics is qualitatively analyzed through Polarized Optical Microscopy (Fig. 4) at 30 °C. The latter is selected by hypothesizing the operative conditions when MPs can be potentially released from mastics after installation.

B50/70 exhibits a brownish hue (Fig. 4a and c), while the ALB displays a yellowish-brown color (Fig. 4d-f). The granular material consists of MPs. HMPs and MMPs are observed to be dispersed as granules within B50/70. In contrast, B50/70+LMPs exhibits distinct morphological characteristics compared to B50/70+HMPs and B50/70+MMPs. The incorporation of LMPs leads to the formation of a strong network structure in the modified bitumen (Fig. 4c). For ALB-based mastics, different results can be noted. All the examined MPs show a granular dispersion in ALB; consequently, they are incapable of forming network structures. It is known that the positive effect of polymers on the base bitumen mainly originates from the physical filling [51] and the network structure formed by MPs and their interaction with the bitumen. More specifically, the incorporation of LMPs enables to form a stable polymer network by reacting with B50/70 through chemical interactions (FTIR spectra in Fig. 5). Conversely, HMPs and MMPs enhance B50/70 primarily through physical filling effects, as no chemical reactions occur; hence, B50/70+LMPs displays the best performance. Additionally, once dispersed, MPs do not form any network within ALB, and no chemical interactions are detected *via* FTIR analysis (Fig. S6, S.M.). Thus, the improvement in performance for albino is largely attributed to the physical filling mechanism of MPs. Among all ALB-based mastics, ALB+HMPs brings the best performance due to the superior dispersion of HMPs in the Albino matrices, characterized by smaller particle size and more uniform distribution compared to MMPs and LMPs [51].

3.2.2. FTIR analysis

FTIR spectra of both MPs and MPs-modified B50/70-based mastics are illustrated in Fig. 5a, c, e in the range of 4000–600 cm^{-1}

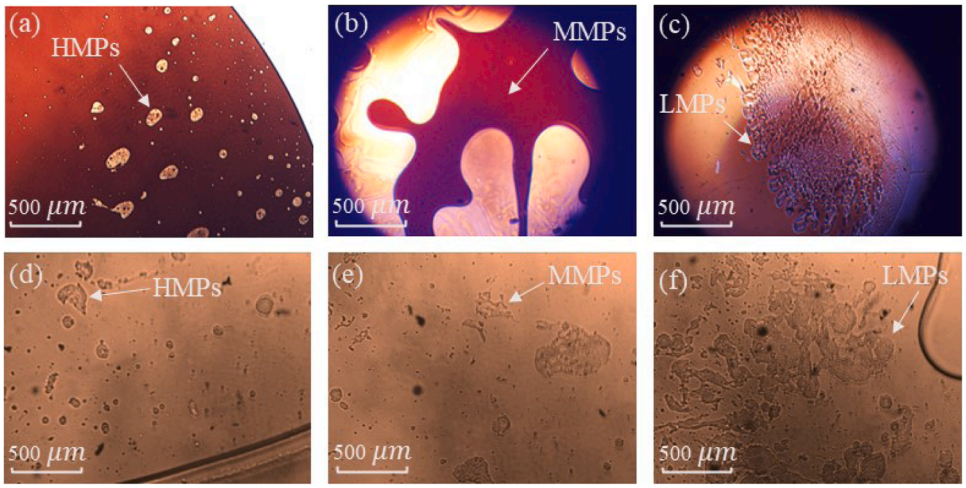

Fig. 4. POM images of B50/70 (a, b, and c) and ALB-based bituminous mastics (d, e, and f) modified with MPs. 10x magnification, scale bar=500 μm.

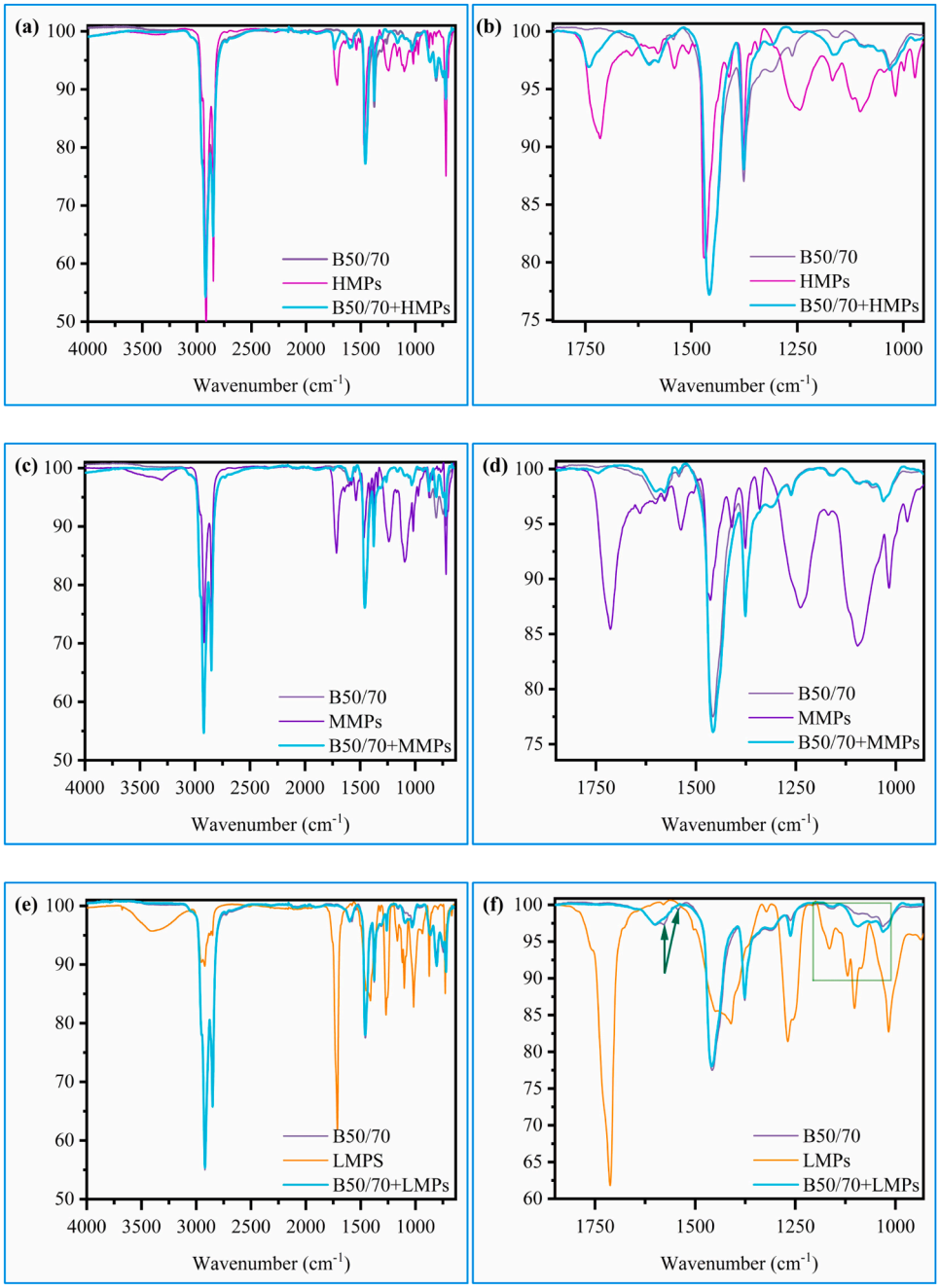

Fig. 5. a-f) FT-IR spectra of B50/70 and B50/70 modified with HMPs (a-b), MMPs(c-d) and LMPs (e-f). b-ᴅ-f) Enlargements of FTIR spectra of B50/70 modified with HMPs (b), MMPs (d) and LMPs (f) in the range of 1760–900 cm^{-1}.

wavenumber. Enlargements of spectra in the range of 1760–900 cm^{-1} are displayed in Fig. 5b, d. FTIR spectra of the selected MPs are shown in Fig. S4 (S.M.). The presence of $C = O$ in the MPs is correlated to the thermal or photo-oxidation of PP [75–77].

The examined spectral region wavenumber takes into account several vibration bands of interest for bitumen i.e. carbonyl ($C = O$, around 1700–1740 cm^{-1}), sulfoxide functional groups ($S = O$ around 1030 cm^{-1}), along with butadiene (-CH═CH-, 960 cm^{-1}) and aromatic groups (around 1605–1570 cm^{-1}) peaks [78–79]. FTIR spectra of LP-modified mastics have already been reported elsewhere [79]; therefore, for brevity, they are not reported here.

FTIR spectra of B50/70 show the following main peaks: aliphatic species (C—H stretching) around 2900 cm^{-1}, the aromatic vibration peaks (ν_{st} $C = C$ ring mode) of the aromatic ring and the secondary amide ($\delta_{i\text{-}p}$ N—H) at 1590 and 1575 cm^{-1} respectively [78,80–82] and the sulfoxide stretching ($S = O$) at 1031 cm^{-1}. On the other hand, for LMPs (Fig. 5e, orange curve), the following vibration peaks are detected: O—H at 3500 cm^{-1} and C—H stretching in the range 2820–3035 cm^{-1} respectively. Furthermore, at 1707 cm^{-1} and around 1100–1150 cm^{-1} the peaks correlated to the free carbonyl group, $C = O$, and the C—O—C bonds can be recognized.

For the case of HMPs (Fig. 5a), the overlapping of all the above-mentioned absorption vibrations is observed. For MMPs (Fig. 5c), the stretching vibration of C—H in the range 2820–3035 cm^{-1}, as well as of that of free carbonyl group $C = O$ at 1716 cm^{-1} along with the C—O—C bonds at 1100–1150 cm^{-1}, are detected. For HMPs and MMPs-modified B50/70 bitumen, the spectra show all the absorption peaks of both bitumen and plastic compounds, respectively, implying that no notable

interaction between bitumen and plastics occurs.

For B50/70+LMPs (Fig. 5e), light blue curve), the FTIR spectra show the disappearance of the carbonyl ($C=O$) stretching band at 1707 cm^{-1}, which is characteristic of the LMPs (likely carboxylic acid or ester groups [76,83]), along with the reduction or disappearance of N–H bending vibrations around 1575 and 1539 cm^{-1}, typically associated with amidic or amine functional groups present in bitumen. These spectral changes suggest the occurrence of chemical interactions between the carbonyl groups of the LMPs and the amidic (or amine) functionalities in bitumen. A plausible mechanism involves the formation of amide or imide linkages through a condensation reaction, where the carboxylic acid or ester groups of the LMPs react with amine groups, releasing water or alcohol as a byproduct. Additionally, a thermally or chemically-induced decarboxylation process, where CO_2 is released, leading to the breakdown or transformation of the carboxylic functional groups, could occur. These interactions are supported by the spectral evolution shown in Fig. 5f, indicating structural modifications and potential chemical integration of LMPs within the bituminous matrix.

FTIR spectra of both MPs and MPs-modified Albino mastics are reported in Fig. S6 (Section S4, S.M.). Also in this case, the main absorption peaks of hydrocarbons can be highlighted i.e. the asymmetric stretching of C—H bonds in the range 2800–2900 cm^{-1}, the stretching of $C=O$ carbonyl at 1742 cm^{-1}, sulfoxide ($S=O$ at 1080 cm^{-1}), along with aromatic groups, (around 1605–1570 cm^{-1}), respectively [78]. However, it must be noticed that FTIR spectra of the examined systems do not differ from each other, and a complete overlap among spectra can be observed. This might be because no chemical interactions take place between the bitumen and MPs, as also pointed out by POM images. In contrast, bare physical interactions occur among MPs and the examined bituminous systems.

3.2.3. Thermal analysis

The thermal properties (T_{onset}, T_{max}) and weight loss and char at 800 °C of MPs and bituminous mastics are summarized in Table 2. Their respective thermal degradation curves are displayed in Fig. S7, S8, S9 (Section S5, S.M.). The temperature at which 5 % weight loss is attained is often considered the onset degradation temperature (T_{onset}) at which the sample starts to decompose [84,85]. T_{max} is the temperature at which the sample undergoes the most rapid thermal degradation, which can be determined from the temperature corresponding to the peak of the DTGA curves. The char residue is calculated as the residual weight upon degradation at 800 °C.

Table 2
Thermal properties of MPs and the examined modified bituminous mastics evaluated by TGA analysis.

(a) MPs

Sample	T_{onset} (°C)	T_{max} (°C)	Weight loss (%)	Char (%)
HMPs	316	468	95.37	4.63
MMPs	354	488	96.71	3.29
LMPs	339	469	84.95	15.05

(b) B50/70-based mastics

Sample	T_{onset} (°C)	T_{max} (°C)	Weight loss (%)	Char (%)
B50/70	345	461	86.68	13.32
B50/70+HMPs	345	467	89.07	10.93
B50/70+MMPs	333	470	91.8	8.20
B50/70+LMPs	344	464	87.35	12.65

(c) ALB-based mastics

Sample	T_{onset} (°C)	T_{max} for stage 1 (°C)	Weight loss for stage 1 (%)	T_{max} for stage 2 (°C)	Weight loss for stage 2 (%)	Char (%)
ALB	273	378	93.17	467	6.551	0.28
ALB+HMPs	283	390	88.11	467	11.45	0.44
ALB+MMPs	282	386	80.77	467	18.56	0.67
ALB+LMPs	298	395	90.93	467	8.532	0.54

T_{onset} of HMPs, MMPs, and LMPs are 316 °C, 354 °C, and 339 °C, respectively (Table 2 a). Both HMPs and MMPs have only one stage of weight loss, occurring at 316 °C-510 °C, corresponding to 92.9 % weight loss, and at 354 °C-521 °C, corresponding to 93.7 % weight loss, respectively. The overall thermal decomposition behavior of LMPs occurs in the range of 339 °C-700 °C, corresponding to 84.6 % weight loss and a T_{max}=469 °C. The latter shows the highest char upon degradation (15 %).

B50/70 presents a first degradation step in 345 °C-550 °C (Fig. S8, Section S5, S.M.), T_{max} of B50/70 is 461 °C with a weight loss of 85.6 %, which is comparable with previous work [78] and with a T_{onset} of 345 °C. T_{onset} of B50/70+HMPs and B50/70+LMPs are 345 °C and 344 °C, respectively, indicating that HMPs and LMPs have no effect on T_{onset} of B50/70 (Fig. S8a, c, d and f, S.M.). In contrast, T_{onset} of B50/70+MMPs (333 °C) is slightly lower than that of neat bitumen thus reducing T_{onset} of B50/70 by 3.5 % (Fig. S8 b and e, S.M.). T_{max} of B50/70+HMPs, B50/70+MMPs, and B50/70+LMPs are slightly higher than that of neat bitumen (467 °C, 470 °C, and 464 °C, respectively, Table 2 b). The char residue also slightly changes using the selected MPs. Overall, for all tested samples, an important degradation event related to the random break/rupture process and subsequent pyrolysis of the components is noticed in agreement with previous works [78].

Fig. S9 (Section S5, S.M.) depicts TGA and DTGA curves of ALB-based mastics made by ALB and HMPs, MMPs, and LMPs. For ALB, two degradation stages can be observed. The first degradation stage takes place between 273 °C and 446 °C (T_{max} equal to 378 °C, Table 2 c); the second degradation stage occurs between 446 °C and 500 °C (T_{max} equal to 467 °C).

T_{max} of ALB+HMPs, ALB+MMPs, and ALB+LMPs are 10 °C, 9 °C, and 25 °C higher than that of ALB (273 °C), respectively (Table 2 c). This result indicates that MPs ensure different degrees of enhancement on the initial degradation temperature of ALB compared to the case of B50/70. In addition, it can be found that MPs do not affect T_{max} of the second degradation stage, whereas, their effect is mainly in the first degradation stage. The char residue is higher than the case of ALB for all examined cases.

From DSC results, two glass transition temperatures (T_g) at −19.3 °C and 31 °C for neat B50/70 bitumen are noted (Fig. S10a and S10b, Section S6, S.M.). The first one might be ascribed to aromatic content, while the second T_g can be correlated to the presence of resins and asphaltenes [81]. But, a T_g at −15.9 °C and T_g = 47 °C and a melting point at 69 °C are recorded for the ALB. By adding the HMPs, MMPs, and LMPs (Fig. S10a, S.M.) in B50/70, an increase of 2.1 %, 5.2 %, and 6.2 % respectively is observed. T_g reflects on the low-temperature performance of asphalt to some extent; lower T_g corresponds to enhanced low-temperature performances of the resulting bituminous mastics [86]. T_g of both B50/70 and ALB increase by adding MPs. This latter aspect indicates that MPs might have some negative effect on the low-temperature properties of bitumen as shown in Nashar et al. [87]. This is in agreement with the performance of MPs-modified mastics in terms of high-frequency (low temperature) rheological properties. In addition, for B50/70+HMPs, B50/70+MMPs, the melting temperature associated with HMPs at 163 °C is also observed. Conversely, for B50/70+LMPs and B50/70+MMPs, the peaks related to the PE plastics (LDPE and LLDPE) disappear. This could be correlated to the chemical interactions between the mastics and MPs, confirming the results of the morphological analysis. It has been demonstrated by [87] that, incorporating a relatively small amount of plastic waste into bitumen (up to 5 wt. %) allows for strong chemical interactions between the plastic waste and bitumen. This is attributed to the low crystallinity of the bituminous system, influenced by the amorphous phase of bitumen. This interaction reduces the melting point of the crystalline regions in the polymeric phase, which corresponds to crystallites with a narrower size distribution. Notably, the system modified with low melting point plastics (LMPs) does not exhibit a melting peak (Fig. S10 a, S.M.), supporting the

hypothesis of high compatibility between the molten MPs and the selected bitumen.

For ALB+HMPs, ALB+MMPs, and ALB+LMPs, T_g increases by 18.9 %, 11.9 %, and 8.8 %, respectively respect to ALB. Furthermore, the melting peak at 69 °C (ALB) and additional melting peaks derived from HMPs (163 °C), MMPs (112 °C, 126 °C and 163 °C), and LMPs (112 °C and 126 °C) are recorded for the resulting modified systems (Fig. S10b, S.M.).

3.3. Leaching tests

Leaching tests in acid solution are performed to study the effect of MPs addition in bituminous mastics. The concentration of Pb, Cd, Co, Ni, and Cu in leachates is evaluated and reported in Fig. 6a and b for B50/70 (a) and ALB (b)-based mastics, respectively.

It is found that leachate contaminant metals such as Ni and Cr are below the detection limits of the ICP instruments, whereas copper and cobalt are observed only in neat bitumen. Considering that bitumen content in asphalts does not exceed 6 % of the total mass, the leachate concentration for all the hazardous metals and in all the analyzed bituminous mastics complies with the law limits [88]. More specifically, the addition of MPs seems to promote a stronger encapsulation of hazardous species within the organic matrix. Therefore, leachate concentration decreases in MPs-modified bituminous mastics, and the best result is attained for the case of Cd, which reduces from 14 mg/kg (neat bitumen) to 2 mg/kg, by employing MMPs in B50/70 (Fig. 6a).

Conversely, in the case of ALB bitumen, Cu, Ni, Mo, and Cr are effectively entrapped within all matrices, while Cd and Pb exhibit reduced concentrations in the leachate solution. This confirms that the inclusion of MPs enhances the immobilization of hazardous species within such a system (Fig. 6b).

Figure S11 (Section S7, S.M.) presents the UV–Vis absorption spectra of eluates from MPs and MPs-based mastics at pH 4. In all cases, the absorbance values are consistently below 0.0001, indicating extremely low concentrations of potential organic pollutants. This strongly suggests that the bituminous mastics modified with marine MPs are environmentally safe, making it suitable for civil engineering applications without posing health risks.

3.4. Life cycle assessment (LCA)

Looking at the LCA [89] results for the overall CC impact indicator (sum of the biogenic, fossil and land use change effects allocated to the 20 years- analysis period) shown in Fig. 7, it might be fair to affirm that the recovery of MPs into bituminous mastics using a B50/70 is environmentally sound in terms of CO_2 eq. reduction compared to the conventional B50/70 + LP manufactured using limestone filler and plain

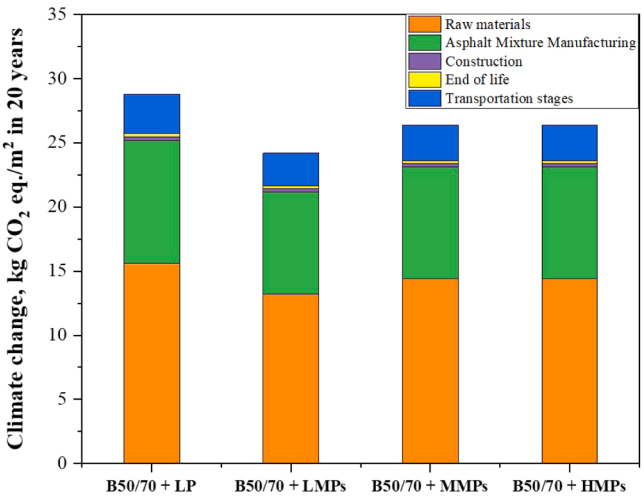

Fig. 7. Life cycle assessment results in terms of Climate Change indicator for 1 m^2 of road base layer in 20 years produced using the asphalt mastics object of the analysis.

50/70 penetration grade bitumen. In detail, the CC indicator decreases, compared to B50/70 + LP, by 15.9 %, 8.3 % and 8.3 % for B50/70 + LMPs, B50/70 + MMPs and B50/70 + HMPs, respectively. The processes affecting the value of the CC indicator are those regarding the production of raw materials, in which the production of limestone filler and the recycling of MPs are included. Comparing the solutions at the raw materials production stage, the recycling process of MPs is equally burdensome as the virgin limestone filler production in terms of CC indicator; the latter accounts for 15.6 kg CO_2 eq./m^2 in 20 years, while MPs recycling produces roughly 15.9 kg CO_2 eq./m^2 in 20 years, with minimum differences mainly accountable to the further recycling process to select LMPs and HMPs from the mixed waste (MMPs). Although the environmental burdens (CC indicator) associated with the production of virgin materials (LP) and the recycling of waste materials (MPs into LMPs, MMPs and HMPs) are not significantly different, the extension of the service life, corroborated by the mechanical tests carried out in the present work, saves the emissions of 4.6 kg CO_2 eq./m^2 in 20 years when the asphalt mastic solution B50/70 + LMPs is adopted instead of B50/70 + LP. Instead, using alternatively the B50/70 + HMPs and B50/70 + MMPs saves about 2.4 kg CO_2 eq./m^2 in 20 years compared to the conventional solution.

In summary, the use of recycled MPs in bitumen is environmentally beneficial mainly because it helps extend the life of the mastic, thus offsetting the initial recycling costs that are comparable to the production of virgin materials.

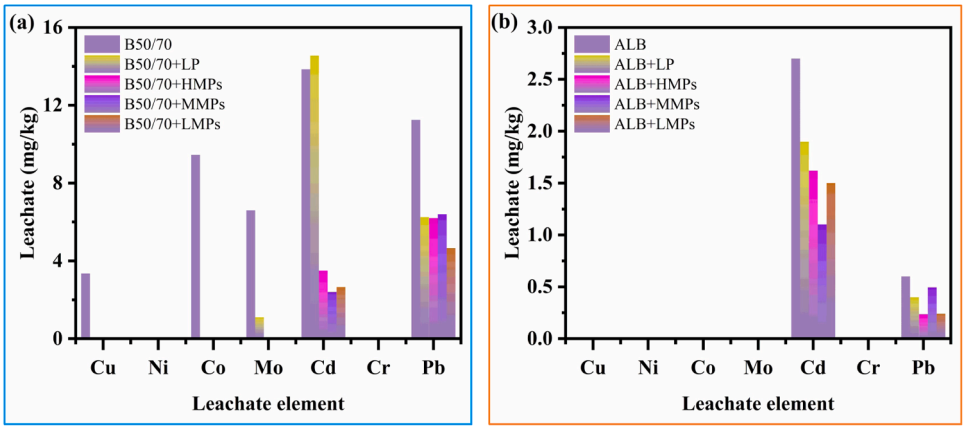

Fig. 6. Results of the leaching test for MPs-modified- B50/70 (a) and ALB (b) bituminous mastics.

4. Conclusions

This study explores using marine microplastics (MPs), specifically those made from PP, PE, and LDPE waste, categorized by their melting points (HMPs, MMPs, and LMPs), as modifiers for two types of bitumen: a standard black bitumen (B50/70) for roads and an eco-friendlier, transparent albino bitumen mastic (ALB) for vehicles pavement application. MPs at 6 wt. % of the bitumen's weight was added to both bitumen. This is the first time marine MPs have been used in bituminous mastics, and in particular, it was assessed their impact on the mastic's basic, rheological, morphological, chemical, and thermal properties. Their performance is compared to conventional limestone powder (LP)-modified mastics. For both bitumen types the environmental impact, including the leaching of heavy metals (using a custom method) and organic compounds (via UV–vis analysis), and a Life Cycle Assessment (LCA) was conducted.

The main conclusions are as follows:

1. Improved Temperature Resistance: Incorporating MPs makes both B50/70 and ALB less sensitive to temperature changes and more resistant to deformation at high temperatures.
2. Enhanced Stiffness and Elasticity: MP-modified mastics generally show higher G* (complex shear modulus), especially at high temperatures, compared to LP-modified mastics. This means MPs improve the bitumen's stiffness and elasticity by reducing its phase angle while increasing G*.
3. Varying Modification Mechanisms:

- LMPs react chemically with B50/70 bitumen, forming a network structure, indicating both chemical and physical modification. However, in ALB, LMPs act as physical fillers, dispersing as particles or flocs.
- HMPs and MMPs physically fill both B50/70 and ALB, dispersing as particles without chemical reactions.

4. Reduced Environmental Impact:

- The modified systems are environmentally friendly, releasing no significant organic compounds.
- Adding MPs to bitumen significantly reduces the leaching of heavy metals. B50/70 mastics modified with MMPs showed the best results, reducing cadmium (Cd) leaching by 85 %.

5. Positive Life Cycle Assessment: A preliminary LCA revealed that while the environmental burden of recycling MPs is similar to extracting and processing limestone in terms of CO_2 equivalent emissions, using LMPs in B50/70 for roads extends the service life, leading to an overall reduction of 4600 kg CO_2 equivalent over 20 years for a 100-meter road section, compared to traditional limestone filler.

These findings suggest that marine MPs are effective and sustainable fillers for bitumen systems in road engineering. However, more research is needed to:

- Quantify the leaching of other potential contaminants from bitumen.
- Refine the LCA boundaries, inventory details, and extend the assessment to other indicators (e.g., mineral, fossil, and energy resource consumption).
- Investigate the effects of different concentrations and types of marine MPs on modified mastic properties, including low-temperature performance through BBR tests.
- Assess the impact of bitumen aging on performance as well as on the leaching behavior, and durability of MP-modified systems.

CRediT authorship contribution statement

Yanqi Wang: Writing – original draft, Validation, Investigation, Data curation, Conceptualization. **Rosa Veropalumbo:** Writing – original draft, Validation, Investigation, Formal analysis, Data curation, Conceptualization. **Federica Recupido:** Writing – original draft, Methodology, Investigation, Formal analysis, Conceptualization. **Cristina Oreto:** Writing – original draft, Validation, Software, Resources, Methodology, Formal analysis, Conceptualization. **Quansheng Sun:** Writing – review & editing, Visualization, Validation, Methodology. **Letizia Verdolotti:** Writing – review & editing, Validation, Resources, Investigation, Funding acquisition, Data curation. **Assunta Campanile:** Writing – original draft, Supervision, Formal analysis, Data curation. **Barbara Liguori:** Writing – review & editing, Validation, Methodology, Formal analysis, Data curation. **Nunzio Viscione:** Validation, Supervision, Methodology, Data curation. **Gianluca Dell'Acqua:** Writing – review & editing, Validation, Supervision, Investigation, Data curation, Conceptualization. **Francesca Russo:** Writing – review & editing, Validation, Methodology, Investigation, Data curation, Conceptualization. **Giuseppe Cesare Lama:** Writing – original draft, Validation, Investigation, Formal analysis, Data curation.

Declaration of competing interest

The authors declare that they have no known competing financial interests or personal relationships that could have appeared to influence the work reported in this paper.

Acknowledgments

This work was supported by the Horizon EU project INTEGRANO project (Multidimensional Integrated Quantitative Approach To Assess Safety And Sustainability Of Nanomaterials In Real Case Life Cycle Scenarios Using Nanospecific Impact Categories, G.A. 101138414).

The authors thank the China Scholarship Council (CSC202206600019). The authors wish to thank Dr. Maria Laura Di Lorenzo (IPCB-CNR) for the acquisition of POM images and Alessandra Aldi, Maria Rosaria Marcedula, and Fabio Docimo (IPCB-CNR) for their technical support in this research.

Supplementary materials

Supplementary material associated with this article can be found, in the online version, at doi:10.1016/j.rineng.2025.106191.

Data availability

Data will be made available on request.

References

[1] Marine plastic debris and microplastics: global lessons and research to inspire action and guide policy change, United Nations Environment Program https://wedocs.unep.org/20.500.11822/7720.
[2] What are the facts? Ocean Plastic pollution explained. (Accessed on 15 th February 2024), https://theoceancleanup.com.
[3] T. Biswas, S.C. Pal, Emerging threats of microplastics on marine environment: a critical review of toxicity measurement, policy practice gap and future research direction, J. Clean. Prod. 434 (2024) 139941, https://doi.org/10.1016/j.jclepro.2023.139941.
[4] A. Thacharodi, R. Meenatchi, S. Hassan, N. Hussain, M.A. Bhat, J. Arockiaraj, H. Hao Ngo, Q. Hoang, A. Pugazhendhi, Microplastics in the environment: a critical overview on its fate, toxicity, implications, management, and bioremediation strategies, J. Env. Manag. 349 (2024) 119433, https://doi.org/10.1016/j.jenvman.2023.119433.
[5] S.K. Bharadwaaj, M. Jaudan, P. Kushwaha, A. Saxena, Exploring cutting-edge approaches in plastic recycling for a greener future, Results Eng. 23 (2024) 102704, https://doi.org/10.1016/j.rineng.2024.102704.
[6] L. Verdolotti, E. Di Maio, G. Forte, M. Lavorgna, S. Iannace, Hydration-induced reinforcement of polyurethane-cement foams: solvent resistance and mechanical

properties, J. Mat. Sci. 45 (12) (2010) 3388–3391, https://doi.org/10.1007/s10853-010-4416-5.
[7] C.G. Avio, S. Gorbi, F. Regoli, Plastics and microplastics in the oceans: from emerging pollutants to emerged threat, Mar. Env. Res. 128 (2017) 2–11, https://doi.org/10.1016/j.marenvres.2016.05.012.
[8] J. Caldwell, L.F. Muff, C.K. Pham, A. Petri-Fink, B. Rothen-Rutishauser, R. Lehner, Spatial and temporal analysis of meso- and microplastic pollution in the Ligurian and Tyrrhenian Seas, Mar. Pollut. Bull. 159 (2020) 111515, https://doi.org/10.1016/j.marpolbul.2020.111515.
[9] A. Ashrafy, A.A. Liza, M.N. Islam, M.M. Billah, S.T. Arafat, M.M. Rahman, M. S. Rahman, Microplastics pollution: a brief review of its source and abundance in different aquatic ecosystems, J. Haz. Mat. Adv. 9 (2023) 100215, https://doi.org/10.1016/j.hazadv.2022.100215.
[10] C.C. Gaylarde, M.P. de Almeida, C.V. Neves, J.A.B. Neto, E.M. da Fonseca, The importance of biofilms on microplastic particles in their sinking behavior and the transfer of invasive organisms between ecosystems, Micro 3 (2023) 320–337, https://doi.org/10.3390/micro3010022.
[11] F. Recupido, M. Petala, S. Caserta, M. Kostoglou, S. Guido, T.D. Karapantsios, Wetting properties of dehydrated biofilms under different growth conditions, Colloids Surf. B Biointerf. 210 (2022) 112245, https://doi.org/10.1016/j.colsurfb.2021.112245.
[12] R. Coyle, G. Hardiman, O. Driscoll, Microplastics in the marine environment: a review of their sources, distribution processes, uptake and exchange in ecosystems. Case stud, Chem. Environ. Eng. 2 (2020) 100010, https://doi.org/10.1016/j.cscee.2020.100010.
[13] P.D. Barai, S.L. Gajbhiye, Y.M. Bhongade, H.S. Kanhere, D.M. Kokare, N.A. Raut, B. A. Bhanvase, S.J. Dhoble, Performance evaluation of existing and advanced processes for remediation of microplastics: a comprehensive review, J. Env. Chem. Eng. 13 (3) (2025) 116194, https://doi.org/10.1016/j.jece.2025.116194.
[14] M. Simon, N. van Alst, J. Vollertsen, Quantification of microplastic mass and removal rates at wastewater treatment plants applying Focal Plane array (FPA)-based fourier Transform infrared (FT-IR) imaging, Water Res. 142 (2018) 1–9, https://doi.org/10.1016/j.watres.2018.05.019.
[15] N. Laskar, U. Kumar, Plastics and microplastics: a threat to environment, Env. Tech. Innov. 14 (2019) 100352, https://doi.org/10.1016/j.eti.2019.100352.
[16] E.M. Duncan, A.C. Broderick, W.J. Fuller, T.S. Galloway, M.H. Godfrey, M. Hamann, C.J. Limpus, P.K. Lindeque, A.G. Mayes, L.C.M. Omeyer, D. Santillo, R.T.E. Snape, B.J. Godley, Microplastic ingestion ubiquitous in marine turtles, Glob. Chang. Biol. 25 (2019) 744–752, https://doi.org/10.1111/gcb.14519.
[17] H.X. Li, L.S. Ma, L. Lin, Z.X. Ni, X.R. Xu, H.H. Shi, Y. Yan, M.Z. Guo, D. Rittschof, Microplastics in oysters *saccostrea cucullata* along the Pearl River Estuary, China. Env. Pollut. 236 (2018) 619–625, https://doi.org/10.1016/j.envpol.2018.01.083.
[18] F. Wu, Y. Wang, J.Y.S. Leung, W. Huang, J. Zeng, Y. Tang, J. Chen, A. Shi, X. Yu, H. Zhang, L. Cao, Accumulation of microplastics in typical commercial aquatic species: a case study at a productive aquaculture site in China, Sci. Total Env. 708 (2020) 135432, https://doi.org/10.1016/j.scitotenv.2019.135432.
[19] A. Alfaro-Núñez, D. Astorga, L. Cáceres-Farías, L. Bastidas, C. Soto Villegas, K. Macay, J.H. Christensen, Microplastic pollution in seawater and marine organisms across the Tropical Eastern Pacific and Galápagos, Sci. Rep. 11 (2021) 6424, https://doi.org/10.1038/s41598-021-85939-3.
[20] M. Carbery, W. O'Connor, T. Palanisami, Trophic transfer of microplastics and mixed contaminants in the marine food web and implications for human health, Env. Int. 115 (2018) 400–409, https://doi.org/10.1016/j.envint.2018.03.007.
[21] Conserve and sustainably use the oceans, seas and marine resources for sustainable development, https://sdgs.un.org/goals/goal14 (Accessed on 3 rd November 2024).
[22] The Ocean Clean-up projects, https://theoceancleanup.com/projects (Accessed on 3 rd November 2024).
[23] Meet the Mr. Trash Wheel Family, https://www.mrtrashwheel.com/trash-wheel-family (Accessed on 3 rd November 2024).
[24] O.C. Basurko, G. Gabiña, A. Andrés M, A. Rubio, I.K. Uriarte, Fishing for floating marine litter in SE Bay of Biscay: review and feasibility study, Mar. Policy 61 (2015) 103–112, https://doi.org/10.1016/j.marpol.2015.07.010.
[25] J. Falk-Andersson, M.L. Haarr, V. Havas, Basic principles for development and implementation of plastic clean-up technologies: what can we learn from fisheries management? Sci. Total Env. 745 (2020) 141117 https://doi.org/10.1016/j.scitotenv.2020.141117.
[26] M. Andres, M. Delpey, I. Ruiz, A. Declerck, C. Sarrade, P. Bergeron, O.C. Basurko, Measuring and comparing solutions for floating marine litter removal: lessons learned in the southeast coast of the Bay of Biscay from an economic perspective, Mar. Policy. 127 (2021) 104450, https://doi.org/10.1016/j.marpol.2021.104450.
[27] F. Russo, C. Oreto, R. Veropalumbo, Promoting resource conservation in road flexible pavement using jet grouting and plastic waste as filler, Res Cons. Rec. 187 (2022) 106633, https://doi.org/10.1016/j.resconrec.2022.106633.
[28] T. Bualuang, P. Jitsangiam, N. Jakrawatana, P. Teeratitayangkul, P. Vongruang, C. Thienchai, P. Wongchana, J. Prommarin, Utilization of plastic waste in hot mix asphalt using dry mixing processes: laboratory assessment of airborne microplastics, Results Eng. 25 (2025) 104464, https://doi.org/10.1016/j.rineng.2025.104464.
[29] Y. Jiang, F. Yang, S.S.U. Hassan Kazmi, Y. Zhao, M. Chen, J. Wang, A review of microplastic pollution in seawater, sediments, and organisms of the Chinese coastal and marginal seas, Chemosphere 286 (2022) 131677, https://doi.org/10.1016/j.chemosphere.2021.131677.
[30] J.W.dos S. Ferreira, J.F.R. Marroquin, J.F. Felix, M.M. Farias, M.D.T. Casagrande, The feasibility of recycled micro polyethylene terephthalate (PET) replacing natural sand in hot-mix asphalt, Constr. Build. Mater. 330 (2022) 127276, https://doi.org/10.1016/j.conbuildmat.2022.127276.
[31] F. Alhomaidat, M.J. Al-Kheetan, S.M. Alosifat, Recycling phosphate mine waste rocks in asphalt mixtures to fully replace natural aggregate: a preliminary study, Results Eng. 25 (2025) 104324, https://doi.org/10.1016/j.rineng.2025.104324.
[32] K. Bailey, K. Sipps, G.K. Saba, G. Arbuckle-Keil, R.J. Chant, N.L. Fahrenfeld, Quantification and composition of microplastics in the Raritan Hudson Estuary: comparison to pathways of entry and implications for fate, Chemosphere 272 (2021) 129886, https://doi.org/10.1016/j.chemosphere.2021.129886.
[33] F. Recupido, G.C. Lama, S. Steffen, C. Dreyer, H. Seidlitz, V. Russo, et al., Efficient recycling pathway of bio-based composite polyurethane foams via sustainable diamine, Ecotox. Env. Saf. 269 (2024) 115758, https://doi.org/10.1016/j.ecoenv.2023.115758.
[34] S. Miri, R. Saini, S.M. Davoodi, R. Pulicharla, S.K. Brar, S. Magdouli, Biodegradation of microplastics: better late than never, Chemosphere 286 (2022) 131670, https://doi.org/10.1016/j.chemosphere.2021.131670.
[35] Y. Wan, X. Chen, Q. Liu, H. Hu, C. Wu, Q. Xue, Informal landfill contributes to the pollution of microplastics in the surrounding environment, Env. Pollut. 293 (2022) 118586, https://doi.org/10.1016/j.envpol.2021.118586.
[36] I.B. Joohari, F. Giustozzi, Chemical and high-temperature rheological properties of recycled plastics-polymer modified hybrid bitumen, J. Clean. Prod. 276 (2020) 123064, https://doi.org/10.1016/j.jclepro.2020.123064.
[37] J. Santos, A. Pham, P. Stasinopoulos, F. Giustozzi, Recycling waste plastics in roads: a life-cycle assessment study using primary data, Sci. Total Env. 751 (2021) 141842, https://doi.org/10.1016/j.scitotenv.2020.141842.
[38] J. De Arimateia Almeida E Silva, L.C. De Figueirêdo Lopes Lucena, J.K. G. Rodrigues, M.W. Carvalho, D.B. Costa, Use of micronized polyethylene terephthalate (PET) waste in asphalt binder, Pet. Sci. Technol. 33 (2015) 1508–1515, https://doi.org/10.1080/10916466.2015.1079538.
[39] J.De A.A.E. Silva, J.K.G. Rodrigues, M.W. De Carvalho, L.C.De F.L. Lucena, E. H. Cavalcante, Mechanical performance of asphalt mixtures using polymer-micronized PET-modified binder, Road Mater. Pavement Des. 19 (2018) 1001–1009, https://doi.org/10.1080/14680629.2017.1283353.
[40] R. Ghabchi, C.P. Dharmarathna, M. Mihandoust, Feasibility of using micronized recycled polyethylene terephthalate (PET) as an asphalt binder additive: a laboratory study, Constr. Build. Mater. 292 (2021) 123377, https://doi.org/10.1016/j.conbuildmat.2021.123377.
[41] B. Singh, L. Kumar, M. Gupta, G.S. Chauhan, Polymer-modified bitumen of recycled LDPE and maleated bitumen, J. Appl. Polym. Sci. 127 (2013) 67–78, https://doi.org/10.1002/app.36810.
[42] M.A. Dalhat, A.Y. Adesina, Utilization of micronized recycled polyethylene waste to improve the hydrophobicity of asphalt surfaces, Constr. Build. Mater. 240 (2020) 117966, https://doi.org/10.1016/j.conbuildmat.2019.117966.
[43] R. Maharaj, C. Maharaj, Physical properties of low-density polyethylene, polyvinylchloride and used engine oil modified asphalt, Prog. Rubber Plast. Tech. 31 (2015) 3, https://doi.org/10.1177/147776061503100303.
[44] D.L. Buruiana, P.L. Georgescu, G.B. Carp, V. Ghisman, Recycling micro polypropylene in modified hot asphalt mixture, Sci. Rep. 13 (2023) 3639, https://doi.org/10.1038/s41598-023-30857-9.
[45] M.A. Dalhat, Water resistance and characteristics of asphalt surfaces treated with micronized-recycled-polypropylene waste: super-hydrophobicity, Constr. Build. Mater. 285 (2021) 122870, https://doi.org/10.1016/j.conbuildmat.2021.122870.
[46] A.H. Albayati, F.S. Mustafa, A.F. Al-ani, M. Sukhija, M.M. Moudhafar, A.M. Maher, Advancing asphalt binder performance through nanomaterial and polymer modification: experimental and statistical insights, Results Eng. 25 (2025) 104458, https://doi.org/10.1016/j.rineng.2025.104458.
[47] M. Machsus, J.H. Chen, D.W. Hayati, M. Khoiri, A.F. Mawardi, R. Basuki, Improvement for asphalt mixture performance using plastic bottle waste, Int. J. GEOMATE. 20 (2021) 139–146, https://doi.org/10.21660/2021.79.j2035.
[48] Y. Duan, K. Wu, C. Serrat, F. Arteaga-Larios, H. Brown, C.J. DuBois, W.G. Buttlar, B. Deng, Assessment of microplastics production from waste plastics-modified asphalt pavement, Res. Cons. Rec. 202 (2024) 107329, https://doi.org/10.1016/j.resconrec.2023.107329.
[49] H. Ibrahim, G. Alam, A. Faheem, Eco-economic analysis of utilizing high volumes of recycled plastic and rubber waste for green pavements: a comparative life cycle analysis, Case. Stud. Cost. Mat. 21 (2024) e03690, https://doi.org/10.1016/j.cscm.2024.e03690.
[50] G. Hao, M. He, S. Mei Lin, G.P. Ong, A. Zulkati, S. Kapilan, Recycling of plastic waste in porous asphalt pavement: engineering, environmental, and economic implications, J. Clean. Prod. 440 (2024) 140865, https://doi.org/10.1016/j.jclepro.2024.140865.
[51] R. Veropalumbo, C. Oreto, N. Viscione, F. Pirozzi, L. Pontoni, G. Trancone, M. Race, F. Russo, Exploring the effect on the environment of encapsulated micro- and nano-plastics into asphalt mastics for road pavement, Env. Res. 216 (2023) 114466, https://doi.org/10.1016/j.envres.2022.114466.
[52] F. Russo, R. Veropalumbo, L. Pontoni, C. Oreto, S.A. Biancardo, N. Viscione, F. Pirozzi, M. Race, Sustainable asphalt mastics made up recycling waste as filler, J. Env. Man 301 (2021) 113826, https://doi.org/10.1016/j.jenvman.2021.113826.
[53] M. Enfrin, R. Myszka, F. Giustozzi, Paving roads with recycled plastics: microplastic pollution or eco-friendly solution? J. Hazard. Mat. 437 (2022) 129334 https://doi.org/10.1016/j.jhazmat.2022.129334.
[54] I. Järlskog, A.M. Strömvall, K. Magnusson, M. Gustafsson, M. Polukarova, H. Galfi, M. Aronsson, Y. Andersson-Sköld, Occurrence of tire and bitumen wear microplastics on urban streets and in sweepsand and washwater, Sci. Total Env. 729 (2020) 138950.

[55] R. Veropalumbo, F. Russo, N. Viscione, S.A. Biancardo, Rheological properties comparing hot and cold bituminous mastics containing jet grouting waste, Adv. Mater. Sci. Eng. (2020) 8078527, https://doi.org/10.1155/2020/8078527.
[56] B. Sengoz, L. Bagayogo, J. Oner, A. Topal, Investigation of rheological properties of transparent bitumen, Constr. Build. Mat. 154 (2017) 1105–1111, https://doi.org/10.1016/j.conbuildmat.2017.07.239.
[57] H.C.A. Brandt, P.C. De Groot, Aqueous leaching of polycyclic aromatic hydrocarbons from bitumen and asphalt, Water Res. 35 (17) (2021) 4200–4207, https://doi.org/10.1016/S0043-1354(01)00216-0.
[58] A. Longo, G. Dal Poggetto, M. Malinconico, P. Laurienzo, E. Di Maio, M.L. Di Lorenzo, Enhancement of crystallization kinetics of poly(L-lactic acid) by grafting with optically pure branches, Polymer 227 (2021) 123852, https://doi.org/10.1016/j.polymer.2021.123852.
[59] A. Salerno, L. Verdolotti, M.G. Raucci, J. Saurina, C. Domingo, R. Lamanna, V. Iozzino, M. Lavorgna, Hybrid gelatin-based porous materials with a tunable multiscale morphology for tissue engineering and drug delivery, Eur. Pol. J. 99 (2018) 230–239, https://doi.org/10.1016/j.eurpolymj.2017.12.024.
[60] L. Verdolotti, E. Di Maio, M. Lavorgna, S. Iannace, L. Nicolais, Polyurethane-cement-based foams: characterization and potential uses, J. Appl. Pol Sci. 107 (1) (2008) 1–8, https://doi.org/10.1002/app.24997.
[61] E. Mansouri, V. Yousefi, V. Ebrahimi, S. Eyvazi, M.S. Hejazi, M. Mahdavi, A. Meshabi, V. Tarhriz, Overview of ultraviolet-based methods used in polycyclic aromatic hydrocarbons analysis and measurement, Sep. Sci. Plus. 3 (2020) 112–120, https://doi.org/10.1002/sscp.201900077.
[62] D. Zhang, B. Birgisson, X. Luo, A new dynamic modulus predictive model for asphalt mixtures based on the law of mixtures, Constr. Build. Mater. 255 (2020) 119348, https://doi.org/10.1016/j.conbuildmat.2020.119348.
[63] D.L. De Jong. Computer program BISAR, layered systems under normal and tangential loads. External Report, Koninklijke/Shell-Laboratorium (1979).
[64] J. Verstraeten, V. Veverka, L. Francken, Rational and practical designs of asphalt pavements to avoid cracking and rutting. In Proceedings, Fifth International Conference on the Structural Design of Asphalt Pavements 1 (1982) 45–58.
[65] K. Ragaert, S. Huysveld, G. Vyncke, S. Hubo, L. Veelaert, J. Dewulf, E.D. Bois, Design from recycling: a complex mixed plastic waste case study, Res. Cons. Rec. 155 (2020) 104646, https://doi.org/10.1016/j.resconrec.2019.104646.
[66] E. Bracquené, M.G. Martinez, E. Wagner, F. Wagner, A. Boudewijn, J. Peeters, J. Duflou, Quantifying the environmental impact of clustering strategies in waste management: a case study for plastic recycling from large household appliances, Waste Manag. 126 (2021) 497–507, https://doi.org/10.1016/j.wasman.2021.03.039.
[67] A.E. Schwarz, T.N. Ligthart, D.G. Bizarro, P. De Wild, B. Vreugdenhil, T. Van Harmelen, Plastic recycling in a circular economy; determining environmental performance through an LCA matrix model approach, Waste Manag. 121 (2021) 331–342, https://doi.org/10.1016/j.wasman.2020.12.020.
[68] A.K. Das, D. Singh, Investigation of rutting, fracture, and thermal cracking behavior of asphalt mastic containing basalt and hydrated lime fillers, Constr. Build. Mater. 141 (2017) 442–452, https://doi.org/10.1016/j.conbuildmat.2017.03.032.
[69] V. Antunes, A.C. Freire, L. Quaresma, R. Micaelo, Influence of the geometrical and physical properties of filler in the filler-bitumen interaction, Constr. Build. Mater. 76 (2015) 322–329, https://doi.org/10.1016/j.conbuildmat.2014.12.008.
[70] B. Xing, W. Fan, C. Zhuang, C. Qian, X. Lv, Effects of the morphological characteristics of mineral powder fillers on the rheological properties of asphalt mastics at high and medium temperatures, Powder Technol. 348 (2019) 33–42, https://doi.org/10.1016/j.powtec.2019.03.014.
[71] J.K. Appiah, V.N. Berko-Boateng, T.A. Tagbor, Use of waste plastic materials for road construction in Ghana. Case stud, Constr. Mater. 6 (2017) 1–7, https://doi.org/10.1016/j.cscm.2016.11.001.
[72] S. Matarneh, N. l Louzi, I. Asi, M. Abdel-Jaber, E. Masad, Effects of nanomodifiers on reological, chemical, and microstructural properties of asphalt mastics, Results Eng. 27 (2025) 105750, https://doi.org/10.1016/j.rineng.2025.105750.
[73] S. Aldagari, S.F. Kabir, E.H. Fini, Investigating aging properties of bitumen modified with polyethylene-terephthalate waste plastic, Res. Cons. Rec. 173 (2021) 105687, https://doi.org/10.1016/j.resconrec.2021.105687.
[74] S. Dessouky, C. Reyes, M. Ilias, D. Contreras, A.T. Papagiannakis, Effect of pre-heating duration and temperature conditioning on the rheological properties of bitumen, Constr. Build. Mater. 25 (2011) 2785–2792, https://doi.org/10.1016/j.conbuildmat.2010.12.058.
[75] Y. Lv, Y. Huang, M. Kong, G. Li, Improved thermal oxidation stability of polypropylene films in the presence of β-nucleating agent, Pol. Test. 32 (2) (2013) 179–186, https://doi.org/10.1016/j.polymertesting.2012.10.008.
[76] I. Weon, Effects of thermal ageing on mechanical and thermal behaviors of linear low density polyethylene pipe Pol, Deg. Stab. 95 (2010) 14–20, https://doi.org/10.1016/j.polymdegradstab.2009.10.016.
[77] L. Costa, M.P. Luda, L. Trossarelli, Ultra high molecular weight polyethylene—II. Thermal- and photo-oxidation, Pol. Deg. Stab. (1997) 41–44, https://doi.org/10.1016/S0141-3910(97)00010-4, 58 (1) (2).
[78] R. Veropalumbo, F. Russo, C. Oreto, G.G. Buonocore, L. Verdolotti, H. Muiambo, S. A. Biancardo, N. Viscione, Chemical, thermal, and rheological performance of asphalt binder containing plastic waste, Sustainability (Switzerland) 13 (24) (2021) 13887, https://doi.org/10.3390/su132413887.
[79] M. Asemani, A.R. Rabbani, Detailed FTIR spectroscopy characterization of crude oil extracted asphaltenes: curve resolve of overlapping bands, J. Pet. Sci. Eng. 185 (2019) 106618, https://doi.org/10.1016/j.petrol.2019.106618.
[80] S. Weigel, D. Stephan, Bitumen characterization with Fourier Transform Infrared spectroscopy and multivariate evaluation: prediction of various physical and chemical parameters, Energy Fuels 32 (2018) 10437–10442, https://doi.org/10.1021/acs.energyfuels.8b02096.
[81] S. Diez, A. Hoefling, P. Theato, W. Pauer, Mechanical and electrical properties of sulfur-containing polymeric materials prepared via inverse vulcanization, Polymers 9 (2) (2017) 59, https://doi.org/10.3390/polym9020059.
[82] T. Xia, W. Chen, J. Xu, Effect of PEG loading on the rheological stability of bitumen/PE/PEG blends based on network structure evolution, Constr. Build. Mater. 237 (2020) 117696, https://doi.org/10.1016/j.conbuildmat.2019.117696.
[83] T. Corrales, F. Catalina, C. Peinado, N.S. Allen, E. Fontain, Photooxidative and thermal degradation of polyethylenes: interrelationship by chemiluminescence, thermal gravimetric analysis and FTIR data, J. PhotoChem. Photobiol. Chem. 147 (3) (2002) 213–224, https://doi.org/10.1016/S1010-6030(01)00629-3.
[84] L. Verdolotti, M. Oliviero, M. Lavorgna, S. Iannace, G. Camino, P. Vollaro, A. Frache, On revealing the effect of alkaline lignin and ammonium polyphosphate additives on fire retardant properties of sustainable zein-based composites, Polym. Degrad. Stab. 134 (2016) 115–125, https://doi.org/10.1016/j.polymdegradstab.2016.10.001.
[85] F. Recupido, G.C. Lama, M. Lavorgna, G.G. Buonocore, R. Marzella, L. Verdolotti, Post-consumer recycling of Tetra Pak®: starting a “new life” as filler in sustainable polyurethane foams, Food Packag. Shelf Life. 40 (2023) 101175, https://doi.org/10.1016/j.fpsl.2023.101175.
[86] A. Samieadel, D. Oldham, E.H. Fini, Multi-scale characterization of the effect of wax on intermolecular interactions in asphalt binder, Constr. Build. Mater. 157 (2017) 1163–1172, https://doi.org/10.1016/j.conbuildmat.2017.09.188.
[87] M. Nashar, T.K. Chaki, S.K. Reddy, Effect of waste plastic as modifier on thermal stability and degradation kinetics of bitumen/waste plastics blend, Thermochim. Acta. 509 (1) (2010) 128–134, https://doi.org/10.1016/j.tca.2010.06.013.
[88] C.J. Spreadbury, K.A. Clavier, A.M. Lin, T.G. Townsend, A critical analysis of leaching and environmental risk assessment for reclaimed asphalt pavement management, Sci. Total Env. 775 (2021) 145741, https://doi.org/10.1016/j.scitotenv.2021.145741.
[89] C. Mourou, A. Bonoli, M. Zamorano, M. Martín-Morales, Environmental impact of roof tiles using recycled waste glass coatings: a Life cycle assessment approach, Build Env. 270 (2025) 112481, https://doi.org/10.1016/j.buildenv.2024.112481.